

This article was downloaded by:

On: 15 January 2011

Access details: *Access Details: Free Access*

Publisher *Taylor & Francis*

Informa Ltd Registered in England and Wales Registered Number: 1072954 Registered office: Mortimer House, 37-41 Mortimer Street, London W1T 3JH, UK



## Journal of Experimental Nanoscience

Publication details, including instructions for authors and subscription information:

<http://www.informaworld.com/smpp/title~content=t716100757>

### Structural and magnetic properties of starch-coated magnetite nanoparticles

T. T. Dung<sup>a</sup>; T. M. Danh<sup>a</sup>; L. T. M. Hoa<sup>b</sup>; D. M. Chien<sup>b</sup>; N. H. Duc<sup>a</sup>

<sup>a</sup> Faculty of Engineering Physics and Nanotechnology, Laboratory for Nano Magnetic Materials and Devices, College of Technology, Vietnam National University, Hanoi, Vietnam <sup>b</sup> Laboratory for Nanotechnology, Vietnam National University, Ho Chi Minh City, Vietnam

**To cite this Article** Dung, T. T. , Danh, T. M. , Hoa, L. T. M. , Chien, D. M. and Duc, N. H.(2009) 'Structural and magnetic properties of starch-coated magnetite nanoparticles', *Journal of Experimental Nanoscience*, 4: 3, 259 – 267

**To link to this Article:** DOI: 10.1080/17458080802570609

**URL:** <http://dx.doi.org/10.1080/17458080802570609>

PLEASE SCROLL DOWN FOR ARTICLE

Full terms and conditions of use: <http://www.informaworld.com/terms-and-conditions-of-access.pdf>

This article may be used for research, teaching and private study purposes. Any substantial or systematic reproduction, re-distribution, re-selling, loan or sub-licensing, systematic supply or distribution in any form to anyone is expressly forbidden.

The publisher does not give any warranty express or implied or make any representation that the contents will be complete or accurate or up to date. The accuracy of any instructions, formulae and drug doses should be independently verified with primary sources. The publisher shall not be liable for any loss, actions, claims, proceedings, demand or costs or damages whatsoever or howsoever caused arising directly or indirectly in connection with or arising out of the use of this material.

## Structural and magnetic properties of starch-coated magnetite nanoparticles

T.T. Dung<sup>a</sup>, T.M. Danh<sup>a\*</sup>, L.T.M. Hoa<sup>b</sup>, D.M. Chien<sup>b</sup> and N.H. Duc<sup>a</sup>

<sup>a</sup>Faculty of Engineering Physics and Nanotechnology, Laboratory for Nano Magnetic Materials and Devices, College of Technology, Vietnam National University, Hanoi, Vietnam;  
<sup>b</sup>Laboratory for Nanotechnology, Vietnam National University, Ho Chi Minh City, Vietnam

(Received 24 April 2008; final version received 21 October 2008)

Magnetic Fe<sub>3</sub>O<sub>4</sub> nanoparticles are prepared by the coprecipitation method and coated with starch as a surfactant. Their structural and magnetic behaviours are studied by means of X-ray diffraction (XRD), Transmission Electron Microscopy (TEM), Raman spectrum, Fourier Transform Infrared (FT-IR) as well as with a Vibrating Sample Magnetometer (VSM). The magnetic Fe<sub>3</sub>O<sub>4</sub> nanoparticles under investigation have an average size of about 14 nm. The coated magnetic nanoparticles exhibit super-paramagnetic behaviours with a blocking temperature of about 170 K and saturation magnetisation ranging between 30 and 50 emu g<sup>-1</sup>. In addition, the results of FT-IR indicated that interactions between the Fe<sub>3</sub>O<sub>4</sub> particles and starch layers are much improved.

**Keywords:** magnetite nanoparticles; surface modification; colloidal stability; magnetic stability

### 1. Introduction

Magnetic nanoparticles have many applications in biomedicine, such as magnetic resonance imaging contrast enhancement, cell separation, hyperthermia and drug delivery, etc. [1,2]. These applications impose strict requirements on the physical, chemical and pharmacological properties of the nanoparticles, including chemical composition, granulometric uniformity, crystal structure, magnetic behaviour, surface structure, adsorption properties, solubility as well as low toxicity. Among magnetic nanoparticles, iron oxide has gained wide attention. These nanoparticles are super-paramagnetic at room temperature; however, due to hydrophobic interactions between the particles, they agglomerate and form large clusters, resulting in an increased particle size and a low colloidal stability. In this case, the clusters exhibit strong magnetic dipole–dipole attractions and show ferromagnetic behaviour [3].

In addition, oxidation can happen with as-prepared magnetite nanoparticles. In order to reinforce the colloidal and magnetic stability, a surface modification with certain long-chain molecules is often indispensable. Practically, high colloidal and magnetic stability was obtained with different polymer surfactants such as poly (D,L lactide-co-glycolide) [4],

---

\*Corresponding author. Email: danhtm@vnu.edu.vn

polymethacrylic acid [5], polyacrylamide [6], polystyrene [7,8], polymethylmethacrylate [9] and polyaniline [10]. Starch can also be used as a functional biocompatible-polymer, which is composed of repeating 1,4- $\alpha$ -D glucopyranosyl units: amylose and amylopectin [11]. The starch presents strong hydrophilic and biodegradable behaviours; hence, it exists in many types of applications.

In this article, a starch-coated magnetite suspension was prepared from the synthesised magnetite and starch solution. The evidence of starch modification in magnetite nanoparticle was evaluated by the Fourier Transform Infrared (FT-IR) spectroscopy. The structural and magnetic properties of starch-coated magnetite nanoparticles are reported.

## 2. Experimental

$\text{Fe}_3\text{O}_4$  magnetic nanoparticles are prepared using the coprecipitation method. The ferric and ferrous chlorides (molar ratio 2: 1) are dissolved in a deoxygenated aqueous solution of HCl. The chemical precipitation is achieved at 25°C under mechanical stirring by adding  $\text{NH}_4\text{OH}$  solution. During the reaction process, the pH is maintained at about 12. The precipitation is washed several times with distilled water, adjusting the pH to neutral, and dried under vacuum at 40°C for 20 h.

Starch solutions with different concentrations are prepared by dissolving starch powders in hot distilled water. The synthesised magnetite was poured into the prepared starch solution under vigorous stirring at 60°C for 2 h. The remaining solution was cooled to room temperature and allows standing for 12 h. The gels formed were washed with distilled water until pH became less than 8. After washing, starch-modified magnetite suspension was prepared by dispersing in deionised water. In this ferrofluid, starch was chemisorbed onto the magnetite nanoparticle surface through their hydroxyl groups by forming interactions with the Fe atoms (Figure 1).

The crystalline structure of the samples was identified from X-ray diffraction (XRD) patterns, taken on a SIEMENS D5000 diffractometer using  $\text{CuK}\alpha$  radiation. The diffraction patterns were carried out in  $2\theta$  mode with step of 0.02° for 1 s. The particle size and morphology were examined by using a transmission electron microscope (TEM). Magnetisation was measured by means of vibrating sample magnetometer (VSM). The zero-field-cooled (ZFC) and field-cooled (FC) cycles were performed by cooling the sample to 77 K at zero field and in the presence of an external field of 100 Oe, respectively.

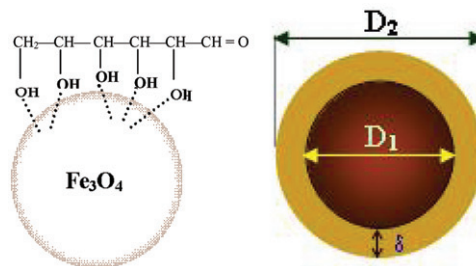


Figure 1. Core-shell structure of starch-coated magnetite nanoparticle.

Fourier Transform Infrared spectroscopy measurements were carried out on a Tensor TM 37 FT-IR spectrometer (Bruker). Pellets for FT-IR analysis were prepared by mixing the lyophilised samples of magnetite nanoparticle formulations with spectroscopic grade KBr powder. A Raman spectrometer (Micro Raman LABRAM 1B) was employed for phase identification.

### 3. Results and discussion

The XRD results of nanoparticles under investigation are illustrated in Figure 2. The patterns are rather pronounced. However, it is difficult to clarify the contribution of magnetite ( $\gamma\text{-Fe}_2\text{O}_3$ ) and magnetite ( $\text{Fe}_3\text{O}_4$ ) from this figure. Fortunately this problem can be solved, thanks to analysis from the Raman spectrum. As can be seen from Figure 3, the Raman spectrum exhibits only three bands at 330, 530 and 670  $\text{cm}^{-1}$ . This is in good corresponding to the  $T_{2g}$ ,  $E_g$  and  $A_{1g}$  Raman bands reported for magnetite by de Faria *et al.* [12]. This means that  $\gamma\text{-Fe}_2\text{O}_3$  and  $\alpha\text{-Fe}_2\text{O}_3$  are not the compositions of our nanoparticles, but it contains magnetite.

The average crystalline size was calculated from the [311] diffraction peaks by using Scherrer's formula as shown [13]:

$$D_c = \frac{0.9\lambda}{L \cdot \cos \theta} \quad (1)$$

where  $D_c$  is the crystalline diameter,  $L$  is the half-intensity width of the diffraction peak,  $\lambda$  is the X-ray wavelength, and  $\theta$  is the angle of the diffraction. It turns out that  $D_c$  is about 10 nm.

The hydrophylic nature of the magnetite nanoparticle surface precludes their dispersal in water. Starch is chemisorbed on the surface of the nanoparticles, which makes the particles hydrophobic, thus these nanoparticles become dispersible in water. The functional groups

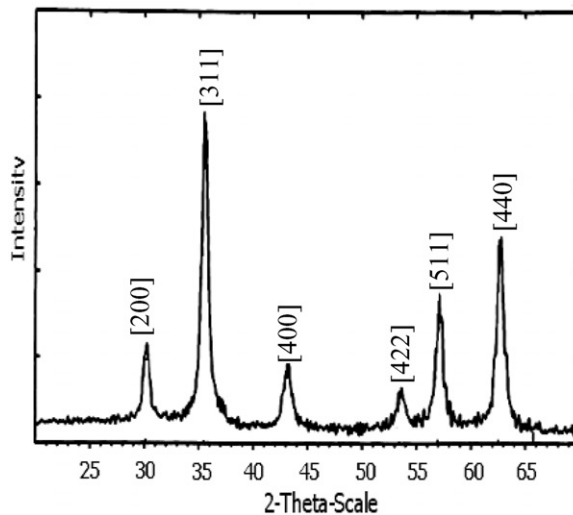


Figure 2. X-ray diffraction patterns of synthesised nanoparticles.

of starch are very important for diverse applications, especially for biotechnology purpose. FT-IR spectroscopy is shown in Figure 4 for pure starch and for 5 and 20 wt% starch-coated magnetite. For pure starch, as clearly seen from Figure 4(a), all of the peaks characterised for the C=O bond, the O–H stretch dimer H-bond, as well as the CH-groups are well appeared in the FT-IR spectra. The spectra of starch-modified magnetite nanoparticles show that both primary groups of starch and magnetite appear in the spectrum (Figure 4(b) and (c)) [14]. The OH-vibration mode, however, is suppressed for the 5 wt% starch-coated magnetite (Figure 4(b)). It suggests the chemisorption of starch onto magnetite nanoparticles through hydroxyl groups (see also Figure 1). At higher starch concentration, e.g., for the 20 wt% starch-coated magnetite, this peak appears again (Figure 4(c)). It may be due to the residual amount of starch in our samples.

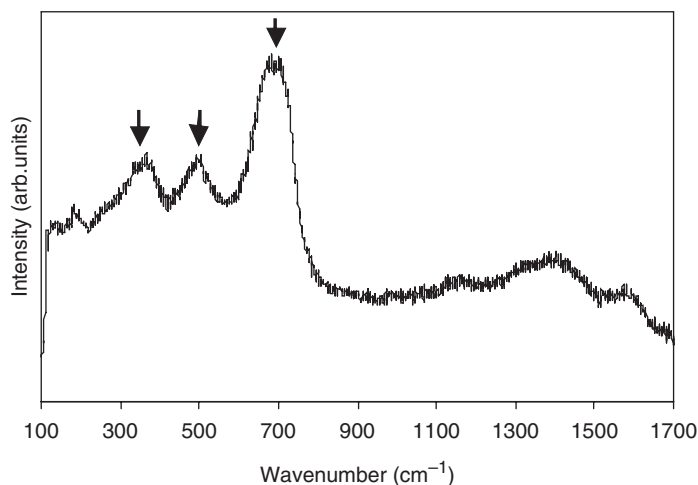


Figure 3. Raman spectra of  $\text{Fe}_3\text{O}_4$  nanoparticles.

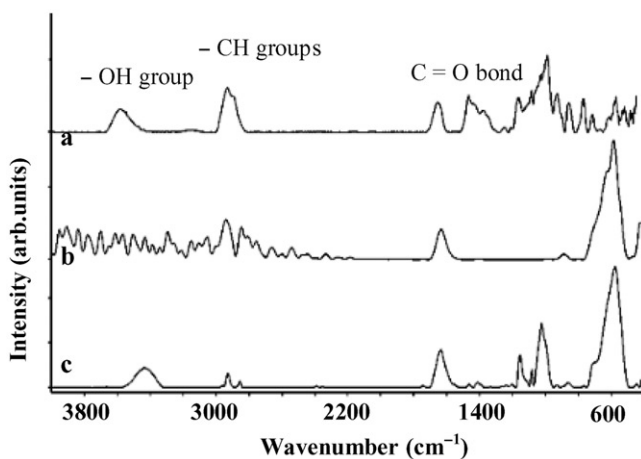


Figure 4. Fourier transform infrared spectra: (a) pure starch, (b) 5 wt% of starch and (c) 20 wt% of starch.

The TEM images of uncoated and coated magnetite are shown in Figure 5. The agglomerated clusters of uncoated magnetite nanoparticles can clearly be seen in Figure 5(a). The starch-coated magnetite nanoparticles are almost spherical, monodisperse with an average diameter  $D_{\text{TEM}} \sim 20$  nm (Figure 5(b)). In addition, the presence of the starch prevents agglomeration of the magnetite nanoparticles. This means that starch chains wrapping around the  $\text{Fe}_3\text{O}_4$  nanoparticles via the interaction between hydroxyl group and iron provide a high colloidal stability. This stability remains even after 6 months.

From the FC and ZFC curves presented in Figure 6, it is clearly seen that the  $\text{Fe}_3\text{O}_4$  sample exhibits a super-paramagnetic behaviour with a blocking temperature of about 170 K. The hysteresis magnetic loops  $M(H)$  measured at 300 K for pure  $\text{Fe}_3\text{O}_4$  and starch-coated  $\text{Fe}_3\text{O}_4$  nanoparticles are shown in Figure 7(a). As seen from this figure, the typical super-paramagnetic characteristics are observed above the blocking temperature. In addition, a decrease of saturation magnetisation ( $M_s$ ) with starch modification is found.

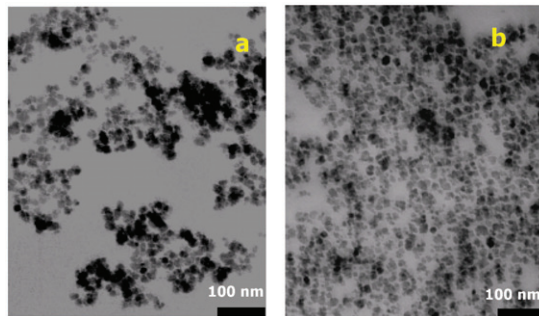


Figure 5. Transmission electron microscopy images of (a) uncoated and (b) starch-coated magnetite.

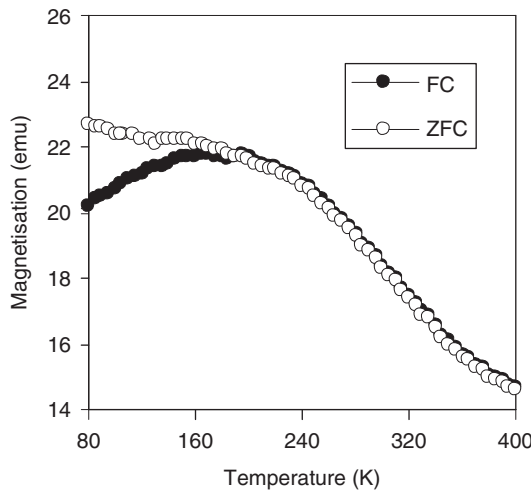


Figure 6. Magnetisation vs. temperature measured at 100 Oe.

This is due to the amount of polymer incorporated in the polymer-coated magnetite suspension. In order to check this argument, the identification of normalised  $M/M_S$  cycles of both magnetite and starch-coated magnetite is presented in Figure 7(b). It proves that surface modification of nanoparticles does not change their intrinsic magnetic behaviour. On the basis of these magnetic data and the average size determined from TEM image

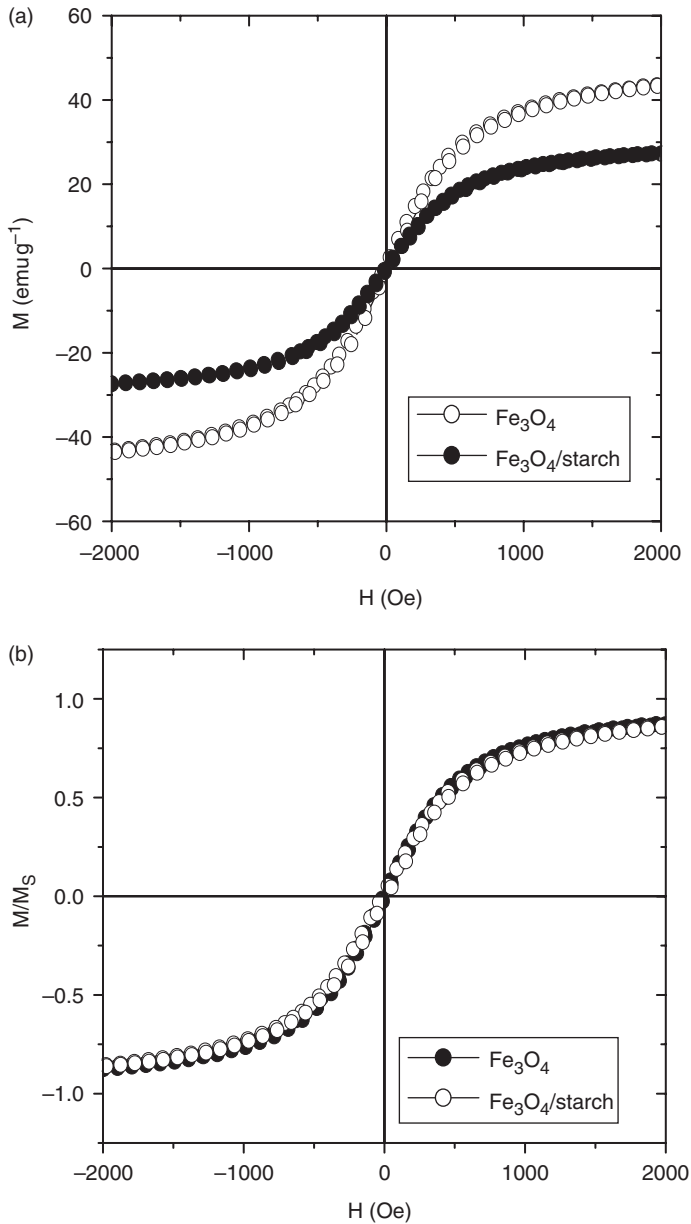


Figure 7. Hysteresis loops of uncoated magnetite and starch-coated magnetite after precipitation.

( $D_{\text{TEM}}$ ), the size of the magnetic core of the particle ( $D_{\text{m}}$ ) is estimated to be about 14 nm. Thus, the starch-layer thickness ( $\delta$ ) is about 3 nm. Note that, the obtained  $D_{\text{m}}$  value is rather close to that of  $D_{\text{c}}$  derived from XRD data.

The magnetic stability (and/or ageing) of magnetite nanoparticles under investigation was verified by comparing the magnetic loops measured at 300 K for specimens kept at normal atmosphere as a function of time. The results are illustrated in Figure 8(a) and (b)

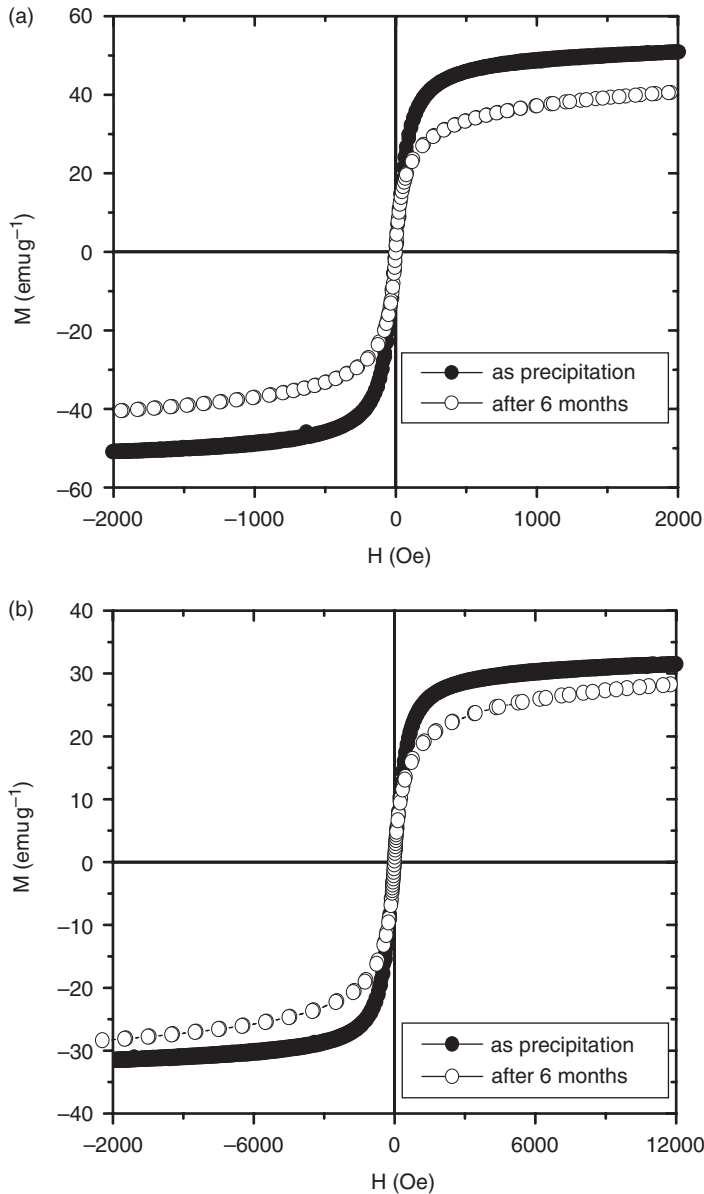


Figure 8. Hysteresis loops of uncoated magnetite (a) and starch-coated magnetite (b) after precipitation and after 6 months.



for the uncoated and starch-coated  $\text{Fe}_3\text{O}_4$  nanoparticles shortly after precipitation and after 6 months. We found that for both samples, the reduction of saturation magnetisation occurs in the first 10 weeks only and after that, no further decrease is observed. For the uncoated sample, the saturation magnetisation decreases from the initially measured  $50\text{--}41 \text{ emu g}^{-1}$  after 6 months; however, the corresponding values are 30 and  $27 \text{ emu g}^{-1}$  for the starch-coated sample. The evolution of the magnetisation with time can be attributed to an increase in the oxide layer on the surfaces, leading to the shrinking of the magnetic core. In this case, it is interesting to emphasise that the starch-coated layer rather well protects them from oxidation and reinforces the magnetic stability. Surface modification of magnetite does not only prevent aggregation and oxidation of magnetite nanoparticles, but also makes them biocompatible. Moreover, the toxicity of the starch-coated magnetite is very low. In a cytotoxic test, Kim *et al.* [15] showed that the validity of L929 cells could be higher than 90% in starch-coated magnetite particles. The exothermic and biocompatible starch-modified magnetite will be selected for an optimised hyperthermic thermoseed.

#### 4. Conclusion

Starch-coated magnetite nanoparticles were prepared and investigated. It is confirmed that starch-coated magnetite nanoparticles have reasonable magnetic properties, high biocompatibility as well as high colloidal and magnetic stability. This suggests that starch-coated magnetite nanoparticles can be considered as one of the bio-potential materials for applications.

#### Acknowledgments

This work was supported by the research project No. QC.08.08 granted by Vietnam National University, Hanoi and the Fundamental Research Program of Vietnam under Project 410.406.

#### References

- [1] P. Reimer and R. Weissleder, [*Development and experimental use of receptor-specific MR contrast media*], *Der Radiologe* 36 (1996), pp. 153–163.
- [2] A. Petri-Fink, M. Chatellain, L. Juilleret-Jeanerret, A. Ferrari, and H. Hofmann, *Development of functionalized superparamagnetic iron oxide nanoparticles for interaction with human cancer cells*, *Biomaterials* 26 (2005), pp. 2685–2694.
- [3] I.W. Hamley, *Nanotechnology with soft materials*, *Angew. Chem. Int. Ed. Engl.* 42 (2003), pp. 692–712.
- [4] S.-J. Lee, J.-R. Jeong, S.-C. Shin, J.-C. Kim, Y.-H. Chang, Y.-M. Chang, and J.-D. Kim, *Nanoparticles of magnetic ferric oxides encapsulated with poly (D,L lactide-co-glycolide) and their applications to magnetic resonance imaging contrast agent*, *J. Magn. Magn. Mater.* 272–276 (2004), pp. 2432–2433.
- [5] H. Zhang, R. Wang, G. Zhang, and B. Yang, *A covalently attached film based on poly(methacrylic acid)-capped  $\text{Fe}_3\text{O}_4$  nanoparticles*, *Thin Solid Films* 429 (2003), pp. 167–173.
- [6] Z.Z. Xu, C.C. Wang, W.L. Yang, Y.H. Deng, and S.K. Fu, *Encapsulation of nanosized magnetic iron oxide by polyacrylamide via inverse miniemulsion polymerization*, *J. Magn. Magn. Mater.* 277 (2004), pp. 136–143.

- [7] Z. Huang, F. Tang, and L. Zhang, *Morphology control and texture of Fe<sub>3</sub>O<sub>4</sub> nanoparticle-coated polystyrene microspheres by ethylene glycol in forced hydrolysis reaction*, *Thin Solid Films* 471 (2005), pp. 105–112.
- [8] Z. Huang and F. Tang, *Preparation, structure, and magnetic properties of polystyrene coated by Fe<sub>3</sub>O<sub>4</sub> nanoparticles*, *J. Colloid Interface Sci.* 275 (2004), pp. 142–147.
- [9] Z.L. Liu, Z.H. Ding, K.L. Yao, J. Tao, G.H. Du, Q.H. Lu, X. Wang, F.L. Gong, and X. Chen, *Preparation and characterization of polymer-coated core-shell structured magnetic microbeads*, *J. Magn. Magn Mater.* 265 (2003), pp. 98–105.
- [10] J. Deng, X. Ding, W. Zhang, Y. Peng, J. Wang, X. Long, P. Li, and A.S.C. Chan, *Magnetic and conducting Fe<sub>3</sub>O<sub>4</sub>-cross-linked polyaniline nanoparticles with core-shell structure*, *Polymer* 43 (2002), pp. 2179–2184.
- [11] M. Avella, J.J. De Vlieger, M.E. Errico, S. Fischer, P. Vacca, and M.G. Volpe, *Biodegradable starch/clay nanocomposites films for food packaging applications*, *Food Chem.* 93 (2005), pp. 467–474.
- [12] D.L.A. de Faria, S. Venancio Silva, and M.T. de Oliveira, *Raman microspectroscopy of some iron oxides and oxyhydroxides*, *J. Raman Spectrosc.* 28 (1997), pp. 873–878.
- [13] C. Hammond, *The Basics of Crystallography and Diffraction*, Oxford University Press, Oxford, 1997.
- [14] J. Li, J. Pan, L. Zhang, X. Guo, and Y. Yu, *Culture of primary rat hepatocytes within porous chitosan scaffolds*, *J. Biomed. Mater. Res.* 67A (2003), pp. 938–943.
- [15] D.H. Kim, S.H. Lee, K.H. Im, K.N. Kim, K.M. Kim, I.B. Shim, M.H. Lee, and Y.K. Lee, *Surface-modified magnetite nanoparticles for hyperthermia: Preparation, characterization, and cytotoxicity studies*, *Current Appl. Phys.* 6(S1) (2006), pp. 242–246.